Journal of Molecular Structure 1178 (2019) 682–691

Contents lists available at ScienceDirect

Journal of Molecular Structure

journal homepage: http://www.elsevier.com/locate/molstruc

Synthetic and structural investigations of Cd(II) complexes of tetradentate pyrimidine based Schiff base ligand: Insight through non-covalent interactions, TDDFT calculation and Hirshfeld surface analysis

Saugata Konar [a, *], Samir Kanti Datta [a], Malay Dolai [b], Amit Das [c], Sudipta Pathak [d], Sudipta Chatterjee [e], Kinsuk Das [f, *]

[a] Department of Chemistry, The Bhawanipur Education Society College, Kolkata, 700020, India
[b] Department of Chemistry, Prabhat Kumar College, Purba Medinipur, 721404, India
[c] Department of Chemistry, Ramsaday College, Amta, Howrah, 711401, India
[d] Department of Chemistry, Haldia Government College, Debhog, Purba Medinipur, West Bengal, 721657, India
[e] Department of Chemistry, Serampore College, Serampore, Hooghly, 712201, India
[f] Department of Chemistry, Chandernagore College, Hooghly, 712136, West Bengal, India

ARTICLE INFO

Article history:
Received 30 July 2018
Received in revised form
20 October 2018
Accepted 23 October 2018
Available online 25 October 2018

Keywords:
Cd(II) complexes
X-ray crystal structures
Supramolecular interactions
TDDFT calculation

ABSTRACT

Two new Cd(II) complexes $[Cd(L)(H_2O)_2]\cdot(ClO_4)_2$ (**1**) and $[Cd(L)(SCN)_2]\cdot(H_2O)$ (**2**) involving pyrimidine based tetradentate schiff base ligand 2,2'-((2E, 2′E)-2,2'-(butane-2,3-diylidene)bis (hydrazin-1-yl-2-ylidene))bis (4,6-dimethylpyrimidine) (**L**) are reported in this work. Both the complexes **1** and **2** are synthesized and characterized by elemental analyses, UV, IR, single crystal X-ray diffraction studies accordingly. Both of them are pseudooctahedral in geometry. In this report we want to highlight the variation of supramolecular non-covalent interactions in the solid state as a consequence of both apical ligand substitution (replacement of neutral aqua molecules by thiocyanate ion) and substitution of noncoordinating anionic counterions by coordinating anions. Complex **1** exhibits H-bonding, π … π stacking, CH … π and anion … π interaction whereas complex **2** displays π … π stacking and CH … π interaction only. The electronic transitions of both **1** and **2** were recorded and the electronic distribution of HOMO - LUMO can be rationalized theoretically (through time-dependent density functional theory (TDDFT)).

1. Introduction

For the last few decades the construction of metal organic framework (MOF s) arrests our interest in the field of research because of their extensive structural variations and potential applications as functional materials [1]. Cd(II) is one of the most toxic anthropogenic pollutants. So, detection, quantification and encapsulation/entrapment of this ion is a significant area of recent research [2–6]. On the other hand the same ion in a suitable coordination environment can exhibit the potentiality in optical and electronic applications. In this respect planning and designing of new pyrimidine based Schiff base ligands have been focused due to their different coordination abilities which in turn reflected in their physicochemical properties. Moreover Pyrimidine is an essential component of many biological active substances. Various pyrimidine derivatives possess antibacterial, antifungal, antimalarial and antitumor activities. The coordination geometry of the complexes depends upon various factors including the size, electronic configuration of the central metal ion as well as the structure, orientation and flexibility of binding sites of the ligand moieties [7,8]. Being d^{10} electronic configuration Cd ((II) does not exhibit any preference to any definite geometrical conformation (as d^{10} configuration is devoid of any CFSE) and hence wide variety of coordination number and as well as their supramolecular architectures have been well studied and reported in the literature [9,10]. Recently we are engaged in studying the coordination behavior of Cd(II) towards some heterocycle based ligands and also pay attention to supramolecular interactions involved in the solid state of the crystals [11,12]. In this paper, we report the syntheses, coordination behavior and electronic properties of two X-ray

* Corresponding authors.
E-mail addresses: saugata.konar@gmail.com (S. Konar), kdaschem@yahoo.in (K. Das).

https://doi.org/10.1016/j.molstruc.2018.10.073
0022-2860/

quality mononuclear Cd(II) complexes derived from a newly synthesized symmetrical tetradentate pyrimidine based Schiff base ligand (2,2'-((2E, 2′E)-2,2'-(butane-2,3-diylidene)bis (hydrazin-1-yl-2-ylidene))bis (4,6-dimethylpyrimidine) **(L)** with symmetrical N4 tetradentate coordination pocket. In complex **1** (1:2 electrolyte) perchlorate ion acts as a non-coordinating counter anions, but when it was treated with thiocyanate ion two axial aqua molecules are replaced by thiocyanate ion (acts as a coordinating anion) to make complex **2** a non-electrolyte one without hampering the equatorial assignment. Linear triatomic pseudohalide thiocyanate coordinates to hard metal centers through the nitrogen end and soft centers *via* the Sulphur end. If the metal centers are borderline like Cd(II), then it can coordinate through either nitrogen or Sulphur atom [13]. If the ancillary ligands increase the electron density on the metal center, then the thiocyanate ion preferentially uses 'S' end in binding to the metal by using the π-acceptor molecular orbital (MO). On the other hand, electron withdrawing ligands decrease the electron density on the metals and thiocyanate ion like to binds through π-donor MO of the 'N' end [14]. It is interesting to note that though Cd(II) is expected to form bond through sulphur end of the thiocyanate ion (due to soft-soft interaction) but as here the pyrimidine derived ligand (**L**) acts as a π-acceptor moiety reinforce the central Cd(II) ion electron deficient and ambidentate thiocyanate ion prefers to form bond with nitrogen end to attain N6 chromophore instead of N4S2.

In the solid state some non-covalent interactions may play a pivotal role to stabilize the crystal structure of the complexes. Now the aim of this report is to elucidate the role of noncovalent interactions on the structural integrity of Cd(II) complexes in presence of non-coordinating (perchlorate aion in complex **1**) and coordinating counter anions (thiocyanate anion in complex **2**) (Scheme 1). Both the complexes have 1D and 2D supramolecular

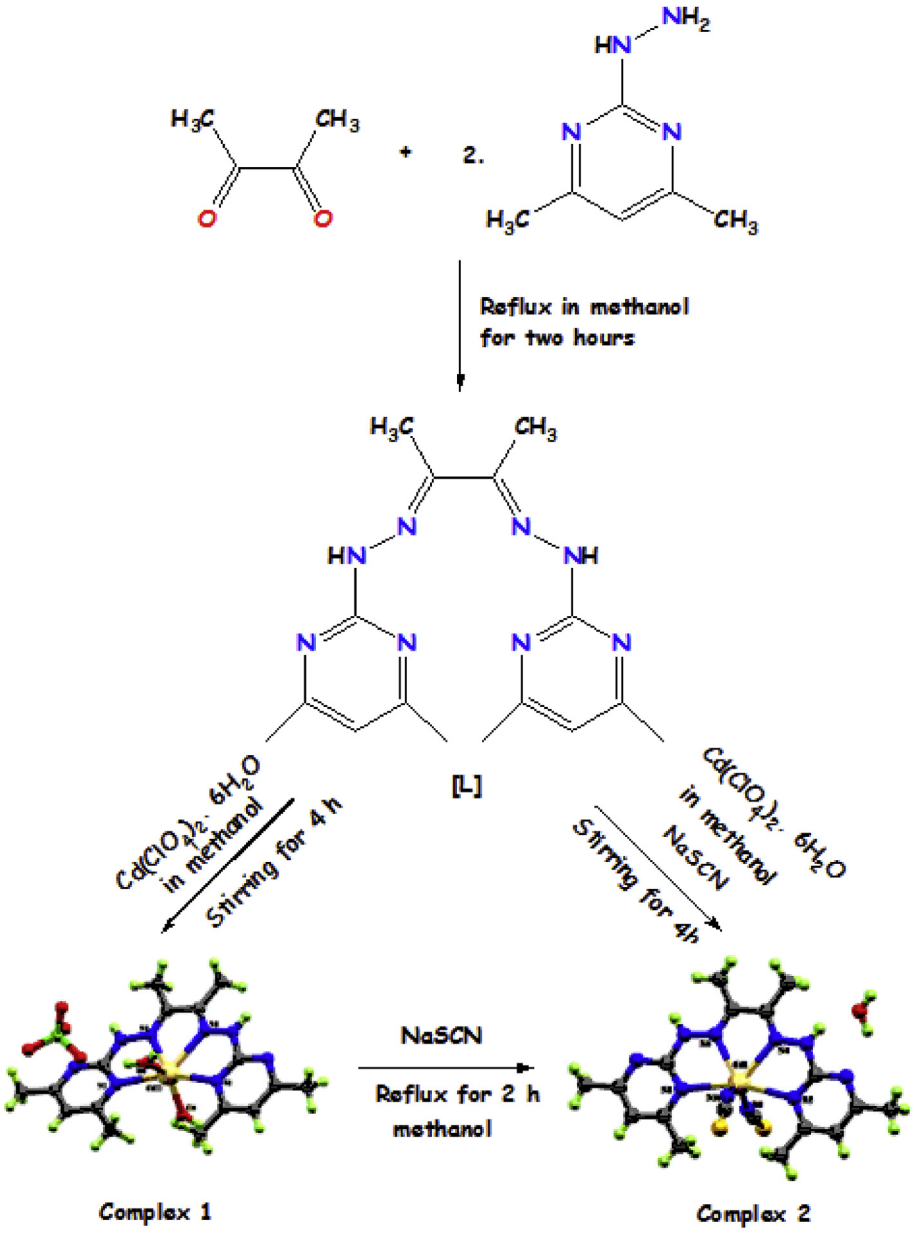

Scheme 1. Schematic diagram of ligand "L" and its Cd(II) complexes.

architecture assisted by non-covalent interactions like H-bonding, π…π stacking, CH…π and anion…π interactions. To understand the electronic structures of these complexes (both **1** and **2)** DFT (Density Functional Theory) calculations have been carried out and furthermore TDDFT (Time Dependent Density Functional Theory) calculations have been done on the DFT optimized geometries, to interpret the electronic transitions accurately.

2. Experimental methods

2.1. General methods and materials

All chemicals were of reagent grade, purchased from commercial sources and used without further purification. 2, 3-Butanedione was purchased from Aldrich Chemical Company, USA and used without further purification.

2.2. Physical measurements

IR spectra were recorded in the region 400–4000 cm^{-1} using a Perkin–Elmer model 883 infrared spectrophotometer. Elemental analysis (C, H and N contents) was carried out by a Perkin–Elmer CHN analyzer 2400 at the Indian Association for the Cultivation of Science, Kolkata. The electronic spectra of the complexes in methanol solution were recorded on a Hitachi model U-3501 spectrophotometer.

2.3. Synthesis

2.3.1. Synthesis of ligand *L [2,2'-((2E,2'E)-2,2'-(butane-2,3-diylidene)bis(hydrazin-1-yl-2-ylidene))bis(4,6-dimethylpyrimidine)]*

The ligand '**L**' was synthesized by refluxing a methanolic solution (30 cm^3) of 2,3-butanedione (0.172 g, 2 mmol) and 2-hydrazino-4,6-dimethyl pyrimidine (0.552 g, 4 mmol) for 2 h (Scheme 1) in presence of two drops of acetic acid. A yellow solid compound is separated out. The solid was filtered off, washed several times with cold methanol and dried in vacuo over fused $CaCl_2$. Yield: 59.0%; Anal. Calcd for $C_{16}H_{22}N_8$: C, 58.88; H, 6.79; N, 34.33%; Found: C, 58.84; H, 6.75; N, 34.38%. ^{1}H NMR (in DMSO-d_6, δ): 10.78 (br s, 2H), 6.39 (s, 2H), 2.20 (s, 12H), 1.24 (s, 6H) (Fig S1). IR (KBr pellet/cm^{-1}): 3271 (m), 1630 (s); 779(m) (Fig S2).

2.3.2. Synthesis of $[Cd(L)(H_2O)_2]\cdot(ClO_4)_2$ *(1)*

A methanolic solution (20 cm^3) of $Cd(ClO_4)_2\cdot 6H_2O$ (1 mmol, 0.419 g) was added dropwise to a solution of **L** (1 mmol, 0.326 g) in the same solvent (20 cm^3) taken in a 1:1 M ratio with constant stirring, and stirring was continued for four additional hours (Scheme 1). The solution turned light yellow and was kept undisturbed for slow evaporation at room temperature. After 1 week X-ray quality crystals of **1** separated out and they were collected by the usual technique. (Yield: 69%). Anal. Calcd for $C_{16}H_{26}CdCl_2N_8O_{10}$ (**1**): C, 28.49; H, 3.85; N, 16.62%; Found: C, 28.44; H, 3.81; N, 16.66%. IR (KBr pellet/cm^{-1}): 3346 (m), 1089 (s), 1622 (s).

2.3.3. Synthesis of $[Cd(L)(SCN)_2]\cdot(H_2O)$ *(2)*

A methanolic solution (20 cm^3) of $Cd(ClO_4)_2\cdot 6H_2O$ (1 mmol, 0.419 g) was added dropwise to a solution of **L** (1 mmol, 0.326 g) in the same solvent (20 cm^3) taken in a 1:1 M ratio with constant stirring, and stirring was continued for two additional hours. The solution turned yellow. To this solution a minimum quantity (4 ml) of an aqueous solution of NaSCN (2 mmol, 0.162 g) was added dropwise to get clear solution, which was stirred for an additional 2 h (Scheme 1). It was left for slow evaporation at room temperature. After 1 week X-ray quality crystals of **2** separated out and they were collected by the usual technique.(Yield: 73%). Elemental analysis: anal. calc. for $C_{18}H_{24}CdN_{10}OS_2$: C, 37.69; H, 4.18; N, 24.43. Found: C, 37.64; H, 4.15; N, 24.45%. IR bands (KBr pellet, cm^{-1}): 2082 (s), 1598 (m), 745 (m). [N.B. Complex **2** can also be synthesized in another method by adding aqueous NaSCN to complex **1** (in methanol solvent) that can be used as a precursor one and continued refluxing for 2 h]

2.4. X-ray crystallography study

Selected crystal data for **1** and **2** are given in Table 1 while their metrical parameters of the complexes are given in Table S1. For **1** and **2** data collections were made using Bruker SMART APEX II CCD

Table 1
Experimental data for crystallographic analysis of complex **1** and **2**.

Complexes	**1**	**2**
Empirical formula	$C_{16}H_{26}CdCl_2N_8O_{10}$	$C_{18}H_{24}CdN_{10}OS_2$
Formula weight	673.75	573.02
Temperature (K)	293 (2)	293 (2)
Crystal system	Monoclinic	Triclinic
Space group	C 2/c	P −1
Unit cell dimensions		
a (Å)	19.863 (4)	9.6904 (4)
b (Å)	10.830 (2)	10.9219 (4)
c (Å)	14.942 (5)	13.1992 (5)
α (°)	90.00	69.746 (2)
β (°)	127.427 (2)	71.717 (2)
γ (°)	90.00	76.517 (2)
Volume ($Å^3$)	2552.6 (11)	1232.21 (8)
Z	4	2
$Density_{cal}$ (Mg m^{-3})	1.753	1.544
Absorption coefficient (mm^{-1})	1.131	1.087
F (000)	1360	580
Independent reflections [R_{int}]	2104 [R (int) = 0.022]	4770 [R (int) = 0.031]
Data/restraints/parameters	2104, 3, 179	4770, 0, 303
Reflections collected	5743	12276
Final R indices [I > 2σ (I)]	R1 = 0.0397, WR2 = 0.1036	R1 = 0.0370, WR2 = 0.1195
Largest difference peak and hole ($eÅ^{-3}$)	−1.01, 0.81	−1.03, 0.99

area detector equipped with graphite monochromated Mo Kα radiation (λ = 0.71073 Å) source in φ and ω scan mode at 293 (2) K for both complexes. Cell parameters refinement and data reduction were carried out using the Bruker SMART APEX II. Cell parameters refinement and data reduction were carried out using Bruker SMART [15] and Bruker SAINT softwares for two complexes. The structures of both complexes were solved by direct and refined by full-matrix least squares based on F^2 using the SHELXS-97 and SHELXL-97 [16] programs.

2.5. Computational details

Ground state electronic structure calculations in gas phase of the complexes (**1** and **2**) have been carried out using DFT [17] method associated with the conductor-like polarizable continuum model (CPCM) [18]. Becke's hybrid function [19] with the Lee-Yang-Parr (LYP) correlation function [20] was used throughout the study. The geometries of the complexes were fully optimized in gas phase without any symmetry constraints. On the basis of the optimized ground state geometry, the absorption spectral properties in methanolic medium were calculated by time-dependent density functional theory (TDDFT) [21] associated with the conductor-like polarizable continuum model. We computed the lowest 40 triplet − triplet transition and results of the TD calculations were qualitatively very similar.

We used 6–31 g as basis set for all the calculations of H, C, N, and O atoms. For Cl, S and Cd atoms we employed 6–31 g + d and GEN as basis set respectively for all the calculations. The calculated electron-density plots for frontier molecular orbitals were prepared by using Gauss View 5.1 software. All the calculations were performed with the Gaussian 09 W software package [22]. Gauss Sum 2.1 program [23] was used to calculate the molecular orbital contributions from groups or atoms.

2.6. Hirshfeld surface analysis

Hirshfeld surfaces [24–26] and the associated 2D-fingerprint [27–29] plots were calculated using Crystal Explorer [30] which accepted a structure input file in CIF format. Bond lengths to hydrogen atoms were set to standard values. For each point on the Hirshfeld isosurface, two distances d_e, the distance from the point to the nearest nucleus external to the surface and d_i, the distance to the nearest nucleus internal to the surface, were defined. The normalized contact distance (d_{norm}) based on d_e and d_i was given by

$$d_{norm} = \frac{(d_i - r_i^{vdw})}{r_i^{vdw}} + \frac{(d_e - r_e^{vdw})}{r_e^{vdw}}$$

where r_i^{vdw} and r_e^{vdw} were the van der Waals radii of the atoms. The value of d_{norm} was negative or positive depending on intermolecular contacts, being shorter or longer than the van der Waals separations. The parameter d_{norm} displayed a surface with a red-white-blue colour scheme, where bright red spots highlighted shorter contacts, white areas represented contacts around the van der Waals separation, and blue regions were devoid of close contacts. For a given crystal structure and set of spherical atomic electron densities, the Hirshfeld surface was unique [31] and it was this property that suggested the possibility of gaining additional insight into the intermolecular interaction of molecular crystals.

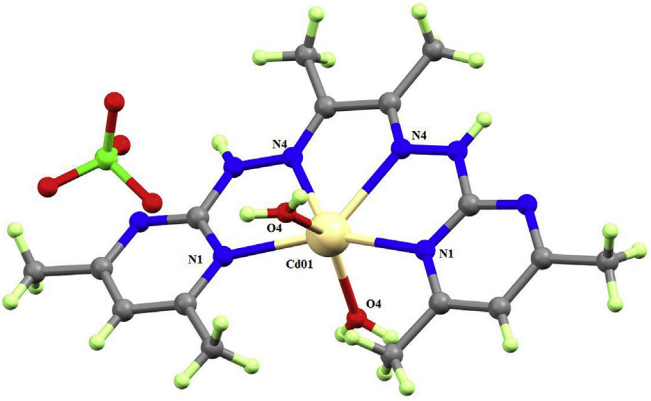

Fig. 1. Molecular structure of **1**.

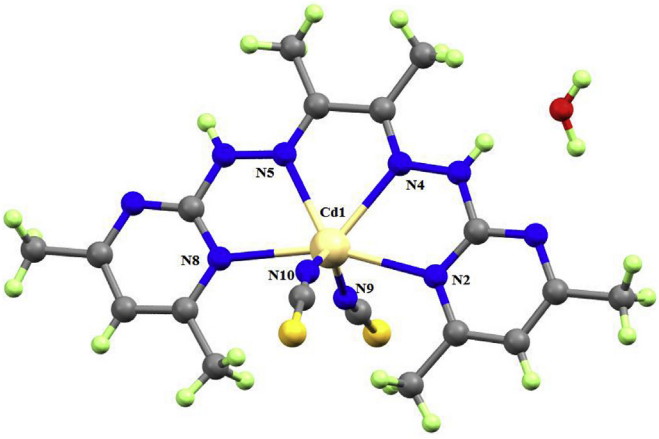

Fig. 2. Molecular structure of **2**.

3. Results and discussion

3.1. Crystal structure descriptions of complexes *1* and *2*

The molecular structures of **1** and **2** with the suitable atom numbering scheme are depicted in Figs. 1 and 2 respectively and selected bond length and bond angle parameters of both **1** and **2** are given in Table S1. The complexes **1** and **2** crystallize in space group C2/c and P-1 respectively. The unit cell of **1** and **2** is comprised of four and two molecules respectively. Structural investigation revealed that in both complexes, the ligand '**L**' serves as a symmetrical tetradentate N4 donor moiety that can be able to bind Cd(II) ion equatorially. The title ligand '**L**' forms three five membered chelate rings on complexation with Cd(II) in both **1** and **2**. Two remaining axial positions are satisfied by two water molecules in **1** and two thiocyanato-N in **2**. $Cd(ClO_4)_2.6H_2O$ is to be used as a source for the metal ion for both complexes. Strategically complex **2** was synthesized in two different ways: first one is by direct metal, ligand and ancillary ligand (here thiocyanate) in 1:1:2 M ratio in methanol and the second route of synthesis is nothing but an axial ligand substitution reaction where two apical aqua molecules of **1** (that can be used here as a precursor for the synthesis of **2**) is replaced by ambidentate pseudohalide thiocyanate ion. In **1**, metal ion adopts a distorted octahedron geometry with a N_4O_2 chromophore. Among four nitrogen atoms two

azomethine nitrogen atoms, N (4), N (4_a), and two pyrimidine nitrogen atoms N (1), N (1_a) of the tetradentate Schiff base ligand define the equatorial periphery at distances of 2.263 (4) Å, 2.263 (4) Å, 2.355 (5) Å, 2.355 (5) Å respectively. Two oxygen atoms [O4 and O4_a] of water molecules are coordinated in the *trans* axial positions at a distance of 2.234 (4) Å. The dipositive charge of the Cd(II) ion is satisfied by two non-coordinated perchlorate giganions. The two axial water molecules along with the central metal ion are a little deviated from an ideal linear arrangement, the angles being 140.38 (12)° due to geometrical restrain. In asymmetric unit, the bond distance C6–N4 1.281 (5) Å is indicative of double bond. The M-ligand average distance of complex is 2.359 Å. The central metal ion sits exactly in the equatorial plane constituted by N1–N4–N4_a-N1_a atoms (no deviation). The geometrical environment around Cd(II) is also distorted octahedron with a N_6 chromophore in **2**. Four nitrogen atoms of which two azomethine nitrogen atoms, N (4), N (5), and two pyrimidine nitrogen atoms N (2), N (8) of the tetradentate Schiff base ligand define the equatorial plane at distances of 2.385 (2) Å, 2.385 (2) Å, 2.464 (3) Å, 2.443 (2) Å respectively. Two coordinated N-bonded thiocyanate ions, N (9) and N (10), are coordinated in the trans axial positions at distances of 2.214 (3) and 2.244 (4)Å. The dipositive charge of the Cd(II) ion is satisfied by two coordinated thiocyanate ions. The sum of the three chelate angles and the non-chelate angle [N8–Cd1–N2] of the octahedral plane is very close to an ideal planar structure for both complexes. The non-chelated angle constituted by two different pyrimidine nitrogen atoms along with the central Cd ((II) ion is deviated much (157.31° for **1** and 159.98° for **2**) from ideal *cis* angle (90°) due to the absence of any spacer. The two axial N-bonded thiocyanate ions including the central metal ions are deviated from a linear arrangement, the angles being 137.74 (13)° due to structural rigidity. The bond distances C9–N5 1.295 (3) Å and C7–N4 1.284 (4) Å are indicative of double bonds. The central metal ion sits in the equatorial plane constituted by N8–N5–N4–N2 atoms by a little deviation (0.036 Å). In contrast to complex **1**, complex **2** is a nonelectrolyte one. As mentioned above second route of the synthesis of **2** is an interconversion of N4O2 to N6 donor environment. Here the thiocyanate ion prefers to coordinate through 'N' end to minimize the steric repulsion provided by the six methyl groups at the peripheral part of the ligand (L). Beside this here the ligand (L) acts as a π-acid one which dictate the Cd(II) metal center to bind with comparatively hard 'N' donor instead of softer 'S' end at the apical site of the distorted octahedron to attain N6 chromophore over N4S2 or N4O2 (in complex **1**). The crystal structure of complex 1in solid state is stabilized by intermolecular H-bonding. There is a hydrogen bonding existing between the hydrogen atom of a coordinated water molecule with the oxygen atom of a perchlorate ion and nitrogen atom of pyrimidine moiety forming 2D network. Details about the H-bonding (Fig. 3) are presented in Table 3. When complex **2** was synthesized from **1** the apical aqua molecules were left from their position to make places for thiocyanato (N-bonded) ion and placed itself into some void places of the crystal which is responsible for weak H-bonding interaction that make a dimeric unit of **2** (Fig. S3, Table 2). In **1** the extension of the dimensionality 2D architecture of H-bonding interaction in **1** is possible due to interaction between non coordinated anion and hydrogen of apical water molecule which is not available in **2** resulting only a dimeric unit of said complex.

3.2. Noncovalent interactions

The complexes **1** and **2** exhibit diverse kinds of weak supramolecular interactions apart from H-bonding like π…π, anion…π and CH…π in solid state structure that contributes to the self-assembly process. For complex **1**, the formation of a

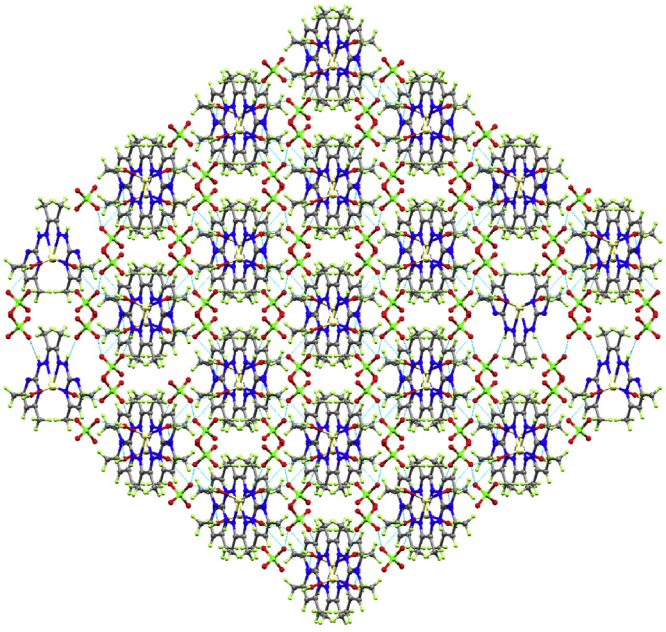

Fig. 3. 2D architecture of H bonding interaction in **1**.

Table 2
Details of hydrogen bond distances (Å) and angles (°) for **1** and **2**.

D H…A	d (D H)	d (H…A)	d (D…A)	<(DHA)
Complex 1				
O4–H2W··· N2	0.83 (5)	2.24 (10)	2.879 (5)	134 (11)
O4–H2W··· O1	0.83 (5)	2.57 (11)	3.099 (10)	123 (10)
N3–H3··· O1	0.8600	2.2000	3.049 (11)	170.00
C7–H7C··· O1	0.9600	2.2800	3.187 (16)	156.00
Complex 2				
N6–H6 ··· O1	0.8600	2.2400	2.911 (4)	135.00
O1–H18 ···N7	0.84 (6)	2.15 (6)	2.992 (4)	178 (7)

D, donor; H, hydrogen; A, acceptor.

supramolecular 1D chain is ensured mostly by two additional π…π interactions (Fig. 4) (Table 3). Firstly, the chelate ring Cg (1) (Cd01–N1–C5–N3–N4) is stacked over the another aromatic ring Cg (4) (N1–C5–N2–C3–C2–C8) of an adjacent molecule of symmetry 1-X,-Y, 2-Z (3.843 (3) Å). Secondly, the aromatic ring Cg (4) (N1–C5–N2–C3–C2–C8) is stacked over the another chelate ring Cg (3) (Cd01–N1_a-C5_a-N3_a-N4_a) adjacent molecule of symmetry X,-Y,-1/2 + Z (3.843 (3) Å). The solid state packing of compound **1** also offers a relevant C–H…π noncovalent interaction (Fig. 5) that is formed between the methyl group of pyrimidine ring (C4–H4C) and the chelate ring Cg (2) (Cd01–N4–C6–C6_a-N4_a)of symmetry related moiety (1-X,-Y, 2-Z) to make 1D crystalline supramolecular building (Table 4). This distance is very short (2.90 Å) signifying a comparative strong interaction. Another type of noncovealent interaction like anion…π is involved in **1** (between noncoordinating O3 and O5 atoms of perchlorate group and pyrimidine ring Cg (4) defined by N1–C5–N2–C3–C2–C8 (of symmetry X,Y,Z) with closest distance of 3.649 (7) Å and 3.072 (7) Å respectively (Fig. S4) (Table 5). Non coordinating perchlorate anion in **1** exhibits anion…π interaction, but in **2** such type of anion…π interaction is absent due to the presence of coordinating anion. Complex **2** shows π…π and CH…π interactions in solid state structure. There are two types of π…π interactions (Fig. 6) (Table S2). Firstly, the chelate ring Cg (1) (Cd (1)-N (2)-C (6)-N (3)-N (4)) is stacked over the same chelate ring Cg (1) of an adjacent

Table 3
Geometric features (distances in Å and angles in degrees) of the π…π interactions obtained for **Complex 1**.

Cg (Ring I)…Cg (Ring J)	Cg…Cg	Cg(I)…Perp	Cg(J)…Perp	α	β	γ	Symmetry
Cg1…Cg4	3.843 (3)	3.421	3.462	3.73	25.74	27.09	1-X,-Y,2-Z
Cg4…Cg3	3.843 (3)	3.421	3.462	3.73	25.74	27.09	X,-Y,-1/2 + Z

α = Dihedral angle between ring I and ring J (°); β = Cg(I)–>Cg(J) or Cg(I)–>Me vector and normal to plane I (°); γ = Cg(I)–>Cg(J) vector and normal to plane J (°); Cg-Cg = Distance between ring Centroids (Å); CgI——Perp = Perpendicular distance of Cg(I) on ring J (Å); CgJ—Perp = Perpendicular distance of Cg(J) on ring I (Å); Cg (1) = centre of gravity of ring [Cd01—N1—N3—N4]; Cg (3) = centre of gravity of ring [Cd01—N1_a-C5_a-N3_a-N4_a] and Cg (4) = centre of gravity of ring [N1—C5—N2—C3—C2—C8].

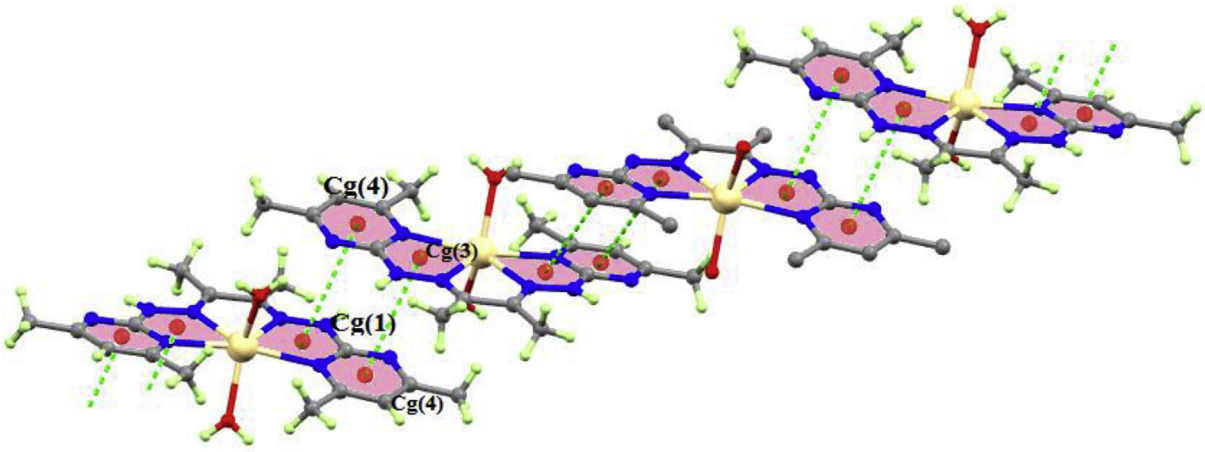

Fig. 4. 1D supramolecular chain generated through π…π interactions in **1** (where, Cg (1) = centre of gravity of ring [Cd01—N1—N3—N4]; Cg (3) = centre of gravity of ring [Cd01—N1_a-C5_a-N3_a-N4_a] and Cg (4) = centre of gravity of ring [N1—C5—N2—C3—C2—C8] and perchlorate molecules are omitted for clarity).

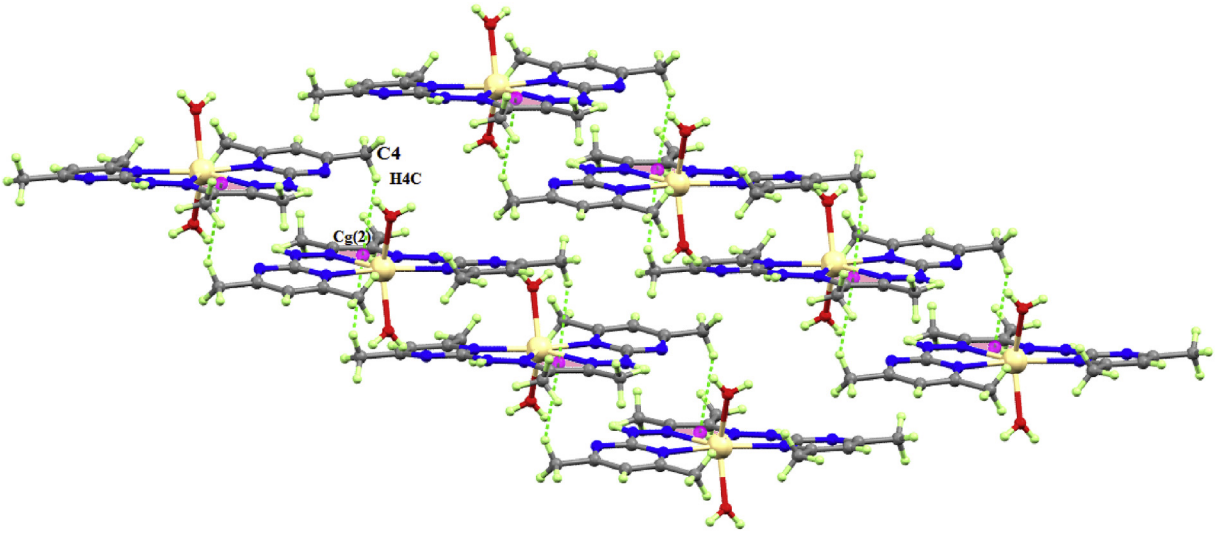

Fig. 5. 1D supramolecular chain generated through C-H…π interactions in 1 (where Cg (2) = centre of gravity of ring [Cd01—N4—C6—C6_a- N4_a] and perchlorate molecules are omitted for clarity).

Table 4
Geometric features (distances in Å and angles in degrees) of the CH…π interaction obtained for **Complex 1**.

C—H…Cg (Ring)	H…Cg (Å)	C—H…Cg (°)	C…Cg (Å)	Symmetry
C4—H4C…Cg2	2.90	147	3.735 (7)	1-X,-Y,2-Z

For **complex 1**, Cg(2) = centre of gravity of ring [Cd01—N4—C6—C6_a- N4_a].

Table 5
Geometric features (distances in Å and angles in degrees) of the anion…π interaction obtained for **Complex 1**.

C—H…Cg (Ring)	H…Cg (Å)	C—H…Cg (°)	C…Cg (Å)	Symmetry
Cl02 —O3…Cg4	3.649 (7)	87.3 (3)	3.850 (3)	X,Y,Z
Cl02 —O5…Cg4	3.072 (7)	114.3 (4)	3.850 (3)	X,Y,Z

For **complex 1**, Cg(4) = centre of gravity of ring [N1—C5—N2—C3—C2—C8].

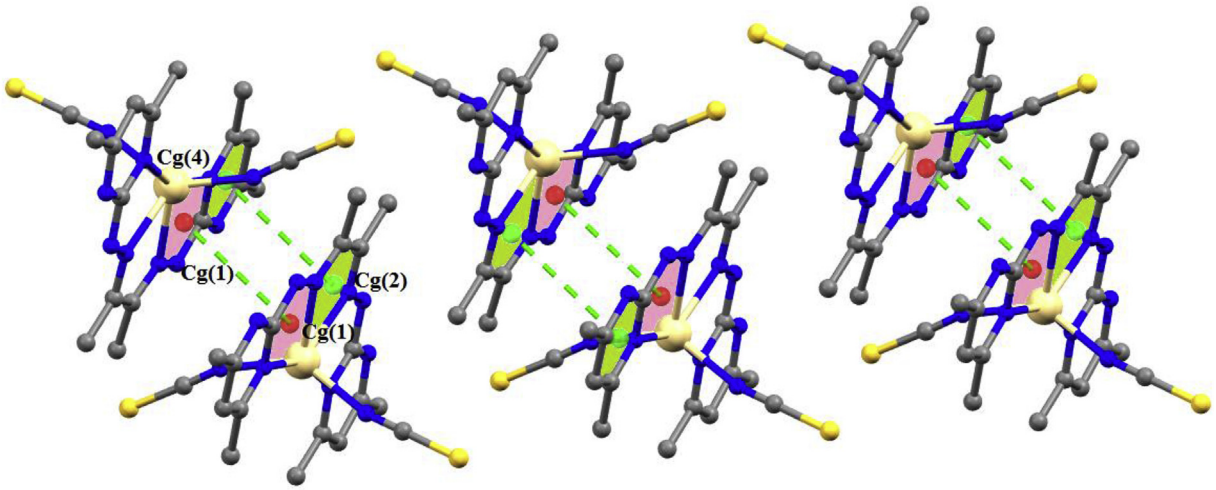

Fig. 6. π…π interactions are involved in **2** (where, Cg (1) = centre of gravity of ring [Cd01–N1–N3–N4]; Cg (2) = centre of gravity of ring [Cd01–N4–C6–C6_a- N4_a] and Cg (4) = centre of gravity of ring [N1–C5–N2–C3–C2–C8] and H-atoms ions are omitted for clarity).

molecule of symmetry 2-X,1-Y, 1-Z (3.7110 (18) Å). Secondly, the chelate ring Cg (2) (Cd (1)-N (4)-C (7)-C (9)-N (5)) is stacked over the another pyrimidine ring Cg (4) (N (1)-C (4)-C (3)-C (2)-N (2)-C (6)) adjacent molecule of symmetry 2-X,1-Y, 1-Z (3.8096 (19) Å). Also, the solid state packing of compound **2** shows a relevant C–H…π noncovalent interaction (Fig. S5) that is formed between the methyl group of pyrimidine ring (C5–H5C) and the pyrimidine ring Cg (5) (N (7)-C (11)-N (8)-C (15)-C (14)-C (12)) of symmetry related moiety (X, 1 + Y,Z) to make 1D crystalline supramolecular building (Table S3).

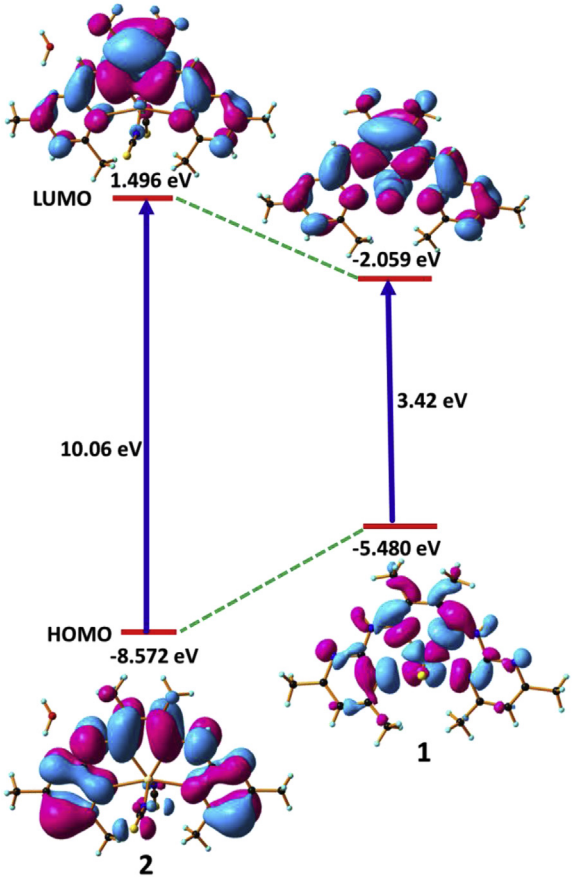

Fig. 7. Frontier molecular orbital of complexes **1** and **2**.

3.3. Geometry optimization and electronic structure

The compositions of the complexes are confirmed by Single Crystal X-ray diffraction studies. We have done the calculations owing the structure from CIF file (from SCXRD). The structures of all the complexes are described above and compared with the optimized geometries of complexes are shown in Fig. 7.

Simultaneously, from TDDFT calculations on **complexes 1** and **2** we got the results of theoretical optical transitions values which are very closely comparable to experimental UV/Vis values (Table S4).

In case of **complex 1**, in the ground state, the electron density resides mainly on HOMO-2, LUMO and LUMO+2 orbital occurs at the phenyl rings along with diacetal, whereas the electron density on LUMO+1, HOMO and HOMO−1 orbital remains at pyrimidinyl nitrogen along with d-orbital of transition metal with an energy gap between HOMO and LUMO of 3.42eV (Fig. 7). In case of **complex 2,** HOMO, LUMO, LUMO+1 and LUMO+2 orbital mainly originates at the phenyl rings along with diacetal, whereas the electron density on HOMO−1 and HOMO−2 orbital remains at d-orbital of transition metal along with thiocyanate ligands with an energy gap between HOMO and LUMO of 10.06eV (Fig. 7).

The UV–Vis absorption spectra of the ligand and its complex (complex 1) were studied at room temperature in MeOH. The ligand shows two well resolved peaks at 225 and 345 nm and the corresponding calculated absorption bands are located at 219 and 342 nm.

These bands are assigned to $S_0 \rightarrow S_{12}$ and $S_0 \rightarrow S_4$ electronic transitions, respectively (Fig. S6). The absorption energies associated with their oscillator strengths are given in Table S4(a).

On the otherhand, **complex 2** shows two absorption bands at 270 and 340 nm (Fig. S7) in MeOH at room temperature and the corresponding calculated absorption bands are located at 265 and 336 nm which are in excellent agreement with experimental re-

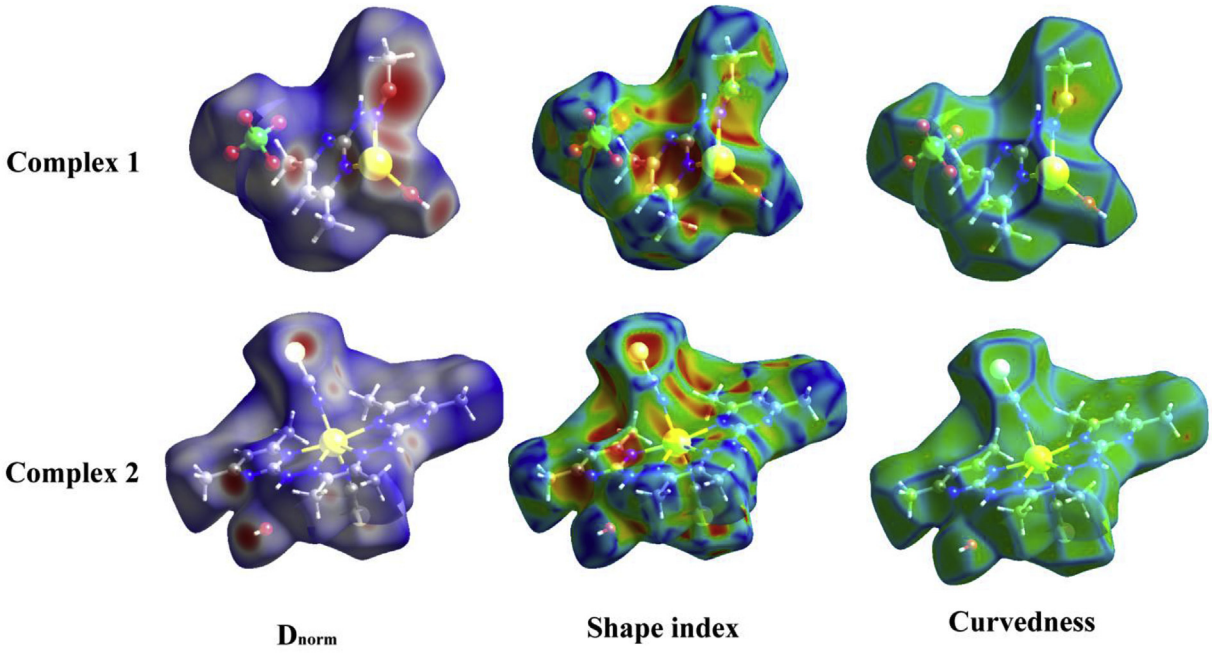

Fig. 8. Hirshfeld surfaces mapped with d_{norm}, shape index and curvedness for complexes **1** and **2**.

sults (Table S4(b). These two absorption bands can be assigned to the $S_0 \rightarrow S_{11}$ and $S_0 \rightarrow S_5$ transitions, respectively (Fig. S7).

3.4. Hirshfeld surface

The Hirshfeld surfaces of both complexes, mapped over d_{norm} (range of −0.1 to 1.5 Å), shape index and curvedness, are illustrated in Fig. 8. The surfaces are shown as transparent to allow visualization of the molecular moiety around which they are calculated. The dominant interaction between O···H/H···O atoms can be seen in the Hirshfeld surfaces as red spots on the d_{norm} surface in Fig. 8. Other visible spots in the Hirshfeld surfaces correspond to N···H and S···H contacts. The small extent of area and light colour on the surface indicates weaker and longer contact other than hydrogen bonds. The intermolecular interactions appear as distinct spikes in the 2D fingerprint plot (Fig. 9). Complementary regions are visible in the fingerprint plots where one molecule acts as donor ($d_e < d_i$) and the other as an acceptor ($d_e > d_i$). The fingerprint plots can be decomposed to highlight particular atoms pair close contacts. This decomposition enables separation of contributions from different interaction types, which overlap in the full fingerprint. The proportions of O···H/H···O interactions comprise 43% and 1.4% of the Hirshfeld surfaces for complexes **1** and **2**, respectively. This O···H/H···O interaction also appears as two distinct spikes in the 2D fingerprint plots (Fig. 9). The lower spike corresponding to the donor spike represents the O···H interactions ($d_i = 1.1$, $d_e = 0.76$ Å in complex **1** and $d_i = 1.5$, $d_e = 1.2$ Å in complex **2**, respectively) and the upper spike being an acceptor spike represents the H···O interactions ($d_i = 0.76$, $d_e = 1.1$ Å in complex **1** and $d_i = 1.2$, $d_e = 1.5$ Å in complex **2**, respectively) in the fingerprint plot (Fig. 9). Similarly the proportion of N···H/H···N interactions comprises 7.8% and 15.6% of the Hirshfeld surfaces for complexes **1** and **2**, respectively. This N···H/H···N interaction also appears as two distinct spikes in the 2D fingerprint plots (Fig. 9). The lower spike corresponding to the donor spike represents the N···H interactions ($d_i = 1.3$, $d_e = 0.9$ Å in complex **1** and $d_i = 1.2$, $d_e = 0.8$ Å in complex **2**, respectively) and the upper spike being an acceptor spike represents the H···N interactions ($d_i = 0.9$, $d_e = 1.3$ Å in complex **1** and $d_i = 0.8$, $d_e = 1.2$ Å in complex **2**, respectively) in the fingerprint plot (Fig. 9). The proportion of S···H/H···S interactions comprises 24.5% of the Hirshfeld surface for complex **2**. Relative contributions to the Hirshfeld surface area for the various intermolecular contacts in both complexes are shown in Fig. 10.

4. Conclusion

We have synthesized two new Cd(II) complexes using a pyrimidine derived symmetrical N4 tetradentate ligand **(L)** [2,2'-((2E, 2′E)-2,2'-(butane-2,3-diylidene)bis (hydrazin-1-yl-2-ylidene))bis (4,6-dimethylpyrimidine)] accompanied by ancillary anionic ligands perchlorate and thiocyanate. Both the complexes (**1** and **2**) are pseudooctahedral and Cd(II) ion is trapped into the equatorial pocket constructed by the N4 moiety of the ligand. Complex **2** was synthesized in two routes: first from direct reactions and the second one by using complex **1** as a precursor one. The second route is more interesting where two axial aqua (neutral) ligands were substituted by two anionic thiocyanate ion keeping the equatorial environment almost same. This type of axial substitution can be reflected in changing the non-covalent interactions in the solid state of the complexes. For better understanding of the electronic

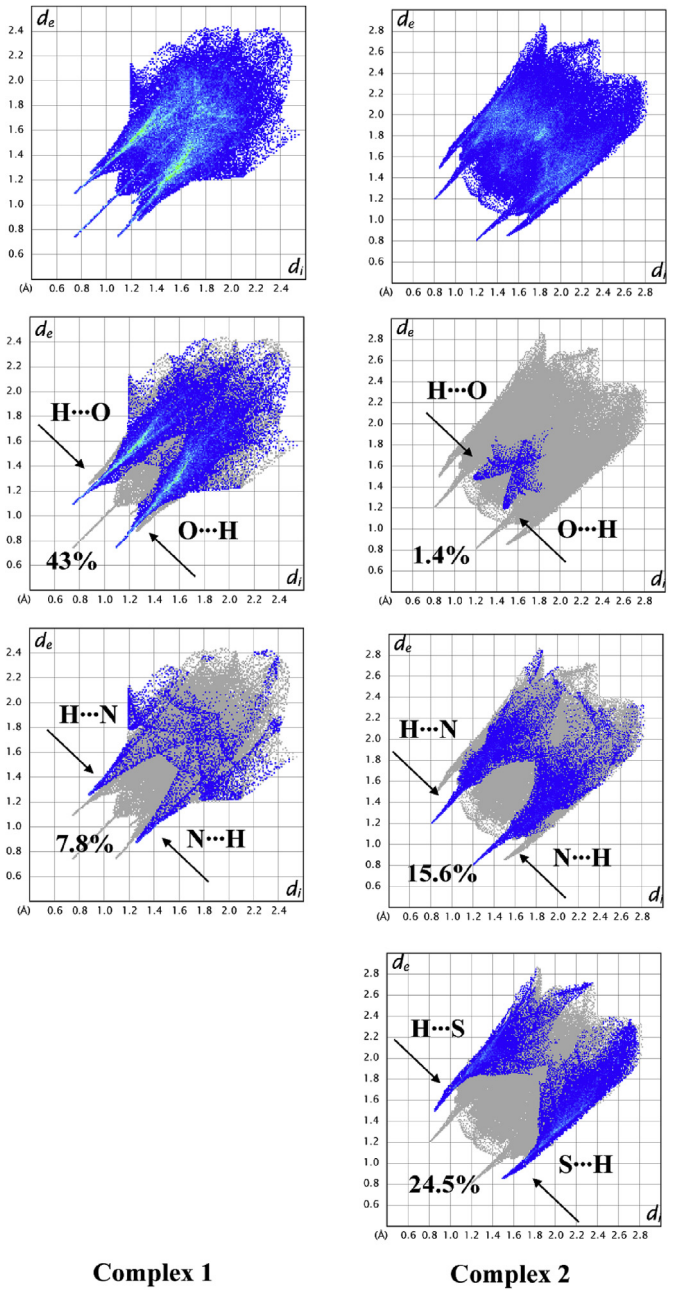

Fig. 9. Fingerprint plots: Full (top), broken down into contributions from specific pair of atom types (below) for complexes **1** and **2**.

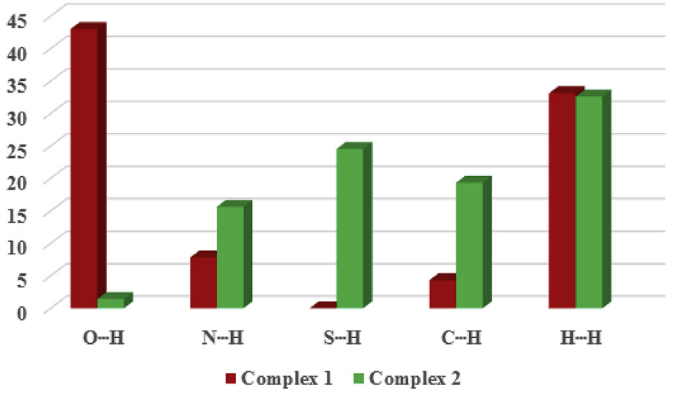

Fig. 10. Relative contribution to the Hirshfeld surface area for the various intermolecular contacts in complexes **1** and **2**.

transitions and the nature of HOMO − LUMO distributions TDDFT (Time Dependent Density Functional Theory) calculations have been carried out on the DFT optimized geometries.

Acknowledgements

S. K. is thankful to The Bhawanipur Education Society College, Kolkata 700020 for providing laboratory space. Authors are also grateful to Sourav Roy and Dr. Shouvik Chattopadhyay, Department of Chemistry, Inorganic Section, Jadavpur University, Kolkata 700032 to help us Hirshfeld surface analysis calculation.

Appendix A. Supplementary data

Supplementary data to this article can be found online at https://doi.org/10.1016/j.molstruc.2018.10.073.

References

[1] B. Xiao, H. Hou, Y. Fan, M. Tang, Impact of counteranion on the self-assembly of Cd(II)-containing MOFs: syntheses, structures and photoluminescent properties, Inorg. Chim. Acta. 360 (2007) 3019–3025, and references therein.

[2] N. Saleh, A.M. Rawashdeh, Y.A. Yousef, Y.A. Al-Soud, Structural characterization of new Cd(2+) fluorescent sensor based on lumazine ligand: AM1 and ab initio studies, Spectrochim. Acta Mol. Biomol. Spectrosc. 68 (2007) 728–733.

[3] H.N. Kim, W.X. Ren, J.S. Kim, J. Yoon, Fluorescent and colorimetric sensors for detection of lead, cadmium, and mercury ions, Chem. Soc. Rev. 41 (2012) 3210–3244.

[4] F. Borbone, U. Caruso, S. Concilio, S. Nabha, S. Piotto, R. Shikler, A. Tuzi, B. Panunzi, From cadmium(II)-aroylhydrazone complexes to metallopolymers with enhanced photoluminescence: a structural and DFT study, Inorg. Chim. Acta. 458 (2017) 129–137.

[5] G. Aragay, J. Pons, A. Merkoçi, Recent trends in macro-, micro-, and nanomaterial-based tools and strategies for heavy-metal detection, Chem. Rev. 111 (2011) 3433–3458.

[6] N. Verma, M. Singh, Biosensors for heavy metals, Biometals 18 (2005) 121–129.

[7] S. Konar, An unprecedented 2D Cd(II) coordination polymer with 3,6 connected binodal net of pyrimidine derived schiff base ligand: synthesis, crystal structure and spectral studies, Inorg. Chem. Commun. 49 (2014) 76–78.

[8] S. Mandal, R. Saha, M. Saha, R. Pradhan, R.J. Butcher, N.C. Saha, Synthesis, crystal structure, spectral characterization and photoluminescence property of three Cd(II) complexes with a pyrazole based Schiff-base ligand, J. Mol. Struct. 1110 (2016) 11–18.

[9] Y.-J. Mu, J.-X. Xie, Y.–G. Ran, B. Han, G.–F. Qin, A series of entangled Cd(II) coordination polymers assembled from different dicarboxylate acids and a flexible imidazole-based ligand, Polyhedron 89 (2015) 20–28.

[10] R. Haldar, S. Bonakala, P. Kanoo, S. Balasubramanian, T.K. Maji, Two 3D metal–organic frameworks of Cd(II): modulation of structures and porous properties based on linker functionalities, Cryst. Eng. Comm. 16 (2014) 4877–4885.

[11] K. Das, S. Konar, A. Jana, A.K. Barik, S. Roy, S.K. Kar, Mononuclear, dinuclear and 1-D polymeric complexes of Cd(II) of a pyridyl pyrazole ligand: syntheses, crystal structures and photoluminescence studies, J. Mol. Struct. 1036 (2013) 392–401.

[12] D. Bose, J. Banerjee, S.H. Rahaman, G. Mostafa, H.K. Fun, D. Rosa, B. Walsh, M.J. Zaworotko, B.K. Ghosh, Polymeric end-to-end bibridged cadmium(II) thiocyanates containing monodentate and bidentate N-donor organic blockers: supramolecular synthons based on π–π and/or C–H···π interactions, Polyhedron 23 (2004) 2045–2053.

[13] A. Hazari, L.K. Das, A. Bauzá, A. Frontera, A. Ghosh, The influence of H-bonding on the 'ambidentate' coordination behaviour of the thiocyanate ion to Cd(II): a combined experimental and theoretical study, Dalton Trans. 43 (2014) 8007–8015.

[14] B. Barszcz, J. Masternak, W.S. Dobrowolska, Assembling novel Cd(II) complexes with multidentate nitrogen donor ligands obtained in situ from the system: zerovalent copper, cadmium oxide, 1-hydroxymethyl-3,5-dimethylpyrazole and ammonium thiocyanate, Dalton Trans. 42 (2013) 5960–5963.

[15] Bruker, SMART v5.631, Bruker AXS Inc., Madison, WI, USA, 2001.

[16] G.M. Sheldrick, SHELXS-97 and SHELXL-97, University of Göttingen, Göttingen, Germany, 1997.

[17] R.G. Parr, W. Yang, Density Functional Theory of Atoms and Molecules, Oxford University Press, Oxford, 1989.

[18] M. Cossi, N. Rega, G. Scalmani, V. Barone, Energies, structures and electronic properties of molecules in solution with the C-PCM solvation model, J. Comput. Chem. 24 (2003) 669–681.

[19] A.D. Becke, Density-functional thermochemistry. III. The role of exact exchange, J. Chem. Phys. 98 (1993) 5648–5652.

[20] C. Lee, W. Yang, R.G. Parr, Development of the Colle-Salvetti correlation-energy formula into a functional of the electron density, Phys. Rev. B 37 (1988) 785–789.
[21] R. Bauernschmitt, R. Ahlrichs, Treatment of electronic excitations within the adiabatic approximation of time dependent density functional theory, Chem. Phys. Lett. 256 (1996) 454–464.
[22] M. J. Frisch, G. W. Trucks, H. B. Schlegel, G. E. Scuseria, M. A. Robb, J. R. Cheeseman, G. Scalmani, V. Barone, B. Mennucci, G. A. Petersson, H. Nakatsuji, M. Caricato, X. Li, H. P. Hratchian, A. F. Izmaylov, J. Bloino, G. Zheng, J. L. Sonnenberg, M. Hada, M. Ehara, K. Toyota, R. Fukuda, J. Hasegawa, M. Ishida, T. Nakajima, Y. Honda, O. Kitao, H. Nakai, T. Vreven, J. A. Montgomery Jr., J. E. Peralta, F. Ogliaro, M. Bearpark, J. J. Heyd, E. Brothers, K. N. Kudin, V. N. Staroverov, R. Kobayashi, J. Normand, K. Raghavachari, A. Rendell, J. C. Burant, S. S. Iyengar, J. Tomasi, M. Cossi, N. Rega, J. M. Millam, M. Klene, J. E. Knox, J. B. Cross, V. Bakken, C. Adamo, J. Jaramillo, R. Gomperts, R. E. Stratmann, O. Yazyev, A. J. Austin, R. Cammi, C. Pomelli, J. W. Ochterski, R. L. Martin, K. Morokuma, V. G. Zakrzewski, G. A. Voth, P. Salvador, J. J. Dannenberg, S. Dapprich, A. D. Daniels, Ö. Farkas, J. B. Foresman, J. V Ortiz, J. Cioslowski and D. J. Fox, Gaussian Inc., 2009, Wallingford CT.
[23] N.M. O'Boyle, A.L. Tenderholt, K.M. Langner, cclib: a library for package-independent computational chemistry algorithms, J. Comput. Chem. 29 (2008) 839–845.
[24] M.A. Spackman, D. Jayatilaka, Cryst. Eng. Comm. 11 (2009) 19–32.
[25] F.L. Hirshfeld, Theor. Chim. Acta 44 (1977) 129–138.
[26] H.F. Clausen, M.S. Chevallier, M.A. Spackman, B.B. Iversen, New J. Chem. 34 (2010) 193–199.
[27] A.L. Rohl, M. Moret, W. Kaminsky, K. Claborn, J.J. McKinnon, B. Kahr, Cryst. Growth Des. 8 (2008) 4517–4525.
[28] A. Parkin, G. Barr, W. Dong, C.J. Gilmore, D. Jayatilaka, J.J. McKinnon, M.A. Spackman, C.C. Wilson, Cryst. Eng. Comm. 9 (2007) 648–652.
[29] M.A. Spackman, J.J. McKinnon, Cryst. Eng. Comm. 4 (2002) 378–392.
[30] S.K. Wolff, D.J. Grimwood, J.J. McKinnon, D. Jayatilaka, M.A. Spackman, Crystal Explorer 2.0, University of Western Australia, Perth, Australia, 2007. http://hirshfeldsurfacenet.blogspot.com.
[31] J.J. McKinnon, M.A. Spackman, A.S. Mitchell, Acta Crystallogr. B 60 (2004) 627–668.